

Radiation from Axion Strings with Adaptive Mesh Refinement: Periodic and Burst Signals

Amelia Drew,^{a,b,*} Tomasz Kinowski^c and E. P. S. Shellard^b

^a*Centre for Theoretical Cosmology, Department of Applied Mathematics and Theoretical Physics, University of Cambridge, Wilberforce Road, Cambridge, CB3 0WA, United Kingdom*

^b*Homerton College, Hills Road, Cambridge, CB2 8PH, United Kingdom*

^c*Gonville and Caius College, Trinity Street, Cambridge, CB2 1TA, United Kingdom*
E-mail: a.drew@damtp.cam.ac.uk, tk593@cam.ac.uk, E.P.S.Shellard@damtp.cam.ac.uk

We present results from investigations of periodic (sinusoidal) and burst signal (colliding travelling wave) configurations of axion strings, performed using adaptive mesh refinement simulations. We model the dependence of the massless axion and massive particle radiation on the amplitude and radius of curvature of the string R . We conclude that the Kalb-Ramond thin-string approximation is valid in the linear regime for sinusoidal strings, and that massive radiation is exponentially suppressed in this regime by parameters that determine the string curvatures i.e. the amplitude A and width of the travelling wave $\sim \sigma_d$. In the nonlinear regime, massless and massive radiation are power-law suppressed with the power law index determined by the ‘regime’ of behaviour, related to the relationship between R , A , δ and σ_d as defined in [1]. For burst signals, in the regime where $R < \sigma_d$ but R is not so low as to form coherent loops, massive particle radiation comprises up to 50% of the total signal. We postulate that this modelling could be usefully incorporated into gravitational wave burst signal predictions and axion spectrum measurements for string networks.

*1st General Meeting and 1st Training School of the COST Action COSMIC WISPerS (COSMICWISPerS)
5-14 September, 2023
Bari and Lecce, Italy*

*Speaker

1. Introduction

Axion strings arise from high energy physics models which incorporate the breaking of a global $U(1)$ symmetry. Motivated by simple extensions to the Standard Model, such as axion dark matter models, grand unified theories and string theory, they arise cosmologically as a result of a ‘phase transition’ in the early Universe and radiate energy via massless axions and massive particles [2]. The mechanism behind these two decay channels is a crucial point of discussion for axion string network evolution and gravitational wave (GW) modelling.

In these proceedings, we outline the methods and main results obtained from parameter scans of sinusoidal and travelling wave axion string configurations, in particular determining the dependence of massive and massless radiation on the string amplitude A and radius of curvature R . Detailed information about this work can be found in [1, 3, 4].

2. Methods

The Lagrangian density \mathcal{L} for the complex scalar field $\varphi = \phi e^{i\theta} = \phi_1 + i\phi_2$ considered is

$$\mathcal{L} = (\partial_\mu \bar{\varphi})(\partial^\mu \varphi) - V(\varphi), \quad (1)$$

with the potential

$$V(\varphi) = \frac{1}{4}\lambda(\bar{\varphi}\varphi - \eta^2)^2. \quad (2)$$

The constant η sets the symmetry breaking scale and the massive particle mass in the broken symmetry state $m_H = \sqrt{\lambda}\eta$. Axion string solutions can be obtained by numerically solving the static Euler-Lagrange equations for the system,

$$\frac{\partial^2 \phi}{\partial r^2} + \frac{1}{r} \frac{\partial \phi}{\partial r} - \frac{1}{r^2} \phi - \frac{1}{2} \phi (\phi^2 - \eta^2) = 0, \quad (3)$$

in cylindrical symmetry, subject to the boundary conditions $\phi(0) = 0$ and $\phi \rightarrow \eta$ as $r \rightarrow \infty$, to obtain the static string profile $\phi(r)$.

We have performed parameter scans over sinusoidal periodic (scan over string width) and analytic travelling wave configurations (scan over amplitude A and approximate width $\sim \sigma_d$) of axion strings. In these proceedings, we focus on the most recent work on burst configurations, obtained by the collision of travelling waves along the string and presented in more detail in [1]. Detailed information about the implementation of sinusoidal configurations can be found in [3, 4].

Analytic travelling wave solutions along an axion string, derived in [5], can be found by redefining $x \rightarrow X$ in the initial data, where the new X -coordinate is given by

$$X = x - \psi(z \pm t). \quad (4)$$

The function $\psi(z \pm t)$ defines the shape of the travelling wave and the direction of travel along the string, in the positive or negative z -direction. We choose to implement two Gaussian travelling waves given by:

$$\psi(z \pm t) = \psi_G(z + t) \pm \psi_G(z - t), \quad (5)$$

where ψ_G is given by

$$\psi_G(z \pm t) = A \exp \left\{ -\frac{(z \pm t \mp b)^2}{2\sigma_d^2} \right\}. \quad (6)$$

Here, A is the amplitude, b is the displacement from the centre of the simulation box at $z = 0$, and σ_d is the standard deviation i.e. approximately the width of the source.

We perform parameter scans of this configuration over initial amplitudes from $0.4 \leq A \leq 35$ with fixed standard deviations $\sigma_d = 2$ and $\sigma_d = 6$, as well as a parameter scan from $1 \leq \sigma_d \leq 6$, with fixed amplitude $A = 5$. In effect, these are scans over the radius of curvature R of the string which determines the string energy per unit length. This is given by

$$\mu \approx \mu_0 + 2\pi\eta^2 \ln(R/\delta), \quad (7)$$

where μ_0 is the contribution from the massive string core and the second term is the contribution from the long-range massless field, with the string width $\delta \sim m_H^{-1}$. The radius of curvature of a Gaussian perturbation of a string, over which we scan in this study, is minimised at its peak with a value of $R_{\text{Gaussian}} = \sigma_d^2/A$. More specific details of the analytic and numerical implementation using the adaptive mesh refinement code GRChombo [6, 7] are given in [1, 3, 4].

To measure the energy radiated by massive and massless radiation, we use the diagnostics

$$E_{\text{massive}} = \int P_{\text{massive}} dt \propto \int (\Pi_\phi \mathcal{D}\phi) \cdot \hat{\mathbf{r}} dS dt, \quad (8)$$

$$E_{\text{massless}} = \int P_{\text{massless}} dt \propto \int (\Pi_\vartheta \mathcal{D}\vartheta) \cdot \hat{\mathbf{r}} dS dt. \quad (9)$$

Here, S is a cylindrical extraction surface around the string and we have defined

$$\Pi_\phi \equiv \dot{\phi} = \frac{\phi_1 \dot{\phi}_1 + \phi_2 \dot{\phi}_2}{\phi}, \quad \mathcal{D}_i \phi \equiv \nabla_i \phi = \frac{\phi_1 \nabla_i \phi_1 + \phi_2 \nabla_i \phi_2}{\phi}, \quad (10)$$

$$\Pi_\vartheta \equiv \phi \dot{\vartheta} = \frac{\phi_1 \dot{\phi}_2 - \phi_2 \dot{\phi}_1}{\phi}, \quad \mathcal{D}_i \vartheta \equiv \phi \nabla_i \vartheta = \frac{\phi_1 \nabla_i \phi_2 - \phi_2 \nabla_i \phi_1}{\phi}. \quad (11)$$

3. Results and Conclusion

Figure 1 shows example evolutions for $A = 4$ and $A = 20$, both with $\sigma_d = 2$. We observe fundamentally different qualitative behaviour of the travelling waves between the two examples. For the lower amplitude $A = 4$, the two travelling waves collide, pass through each other and move apart, with internal mode oscillations generated at the point of collision continuing to radiate over time. For the highly nonlinear $A = 20$, the travelling waves have sufficient energy at the point of collision that they instantaneously create an additional loop of string. The loop reconnects with the long string such that the central portion of the string is displaced. The extreme topological regime at very high amplitude is therefore fundamentally different from the behaviour we observe in the other regimes, even compared to other nonlinear configurations.

Figure 2 gives two examples of the quantitative results obtained from the parameter scans, specifically $1 \leq \sigma_d \leq 6$ with $A = 5$ and $0.4 \leq A \leq 35$ with $\sigma_d = 2$. We observe that in the first scan over

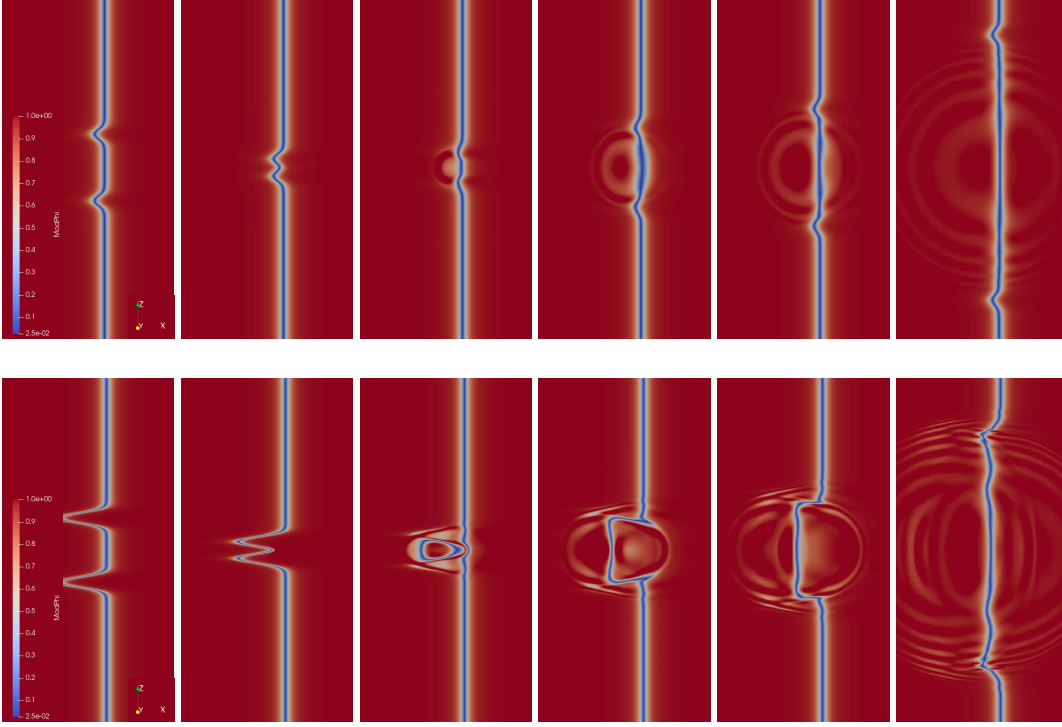


Figure 1: 2D slices of $|\phi|$ for Gaussian/Gaussian travelling wave configurations over time, running from left to right. The top row shows $A = 4$ and $\sigma_d = 2$, and the bottom row is $A = 20$ and $\sigma_d = 2$

an approximately linear regime, the massive radiation is exponentially suppressed with R_{Gaussian} , specifically with σ_d , and the massless radiation is approximately independent of σ_d . For the second scan within the highly nonlinear regime, we observe that both massive and massless radiation are power-law suppressed with approximately equivalent power law indices. The low amplitude region on the right of the plot of the nonlinear regime can be fitted to $E \propto A^4$ for both channels, and the higher amplitude region to $E \propto A^2$. In the lower amplitude region here, the massive and massless signals are of approximately equal magnitude.

We conclude that the characterisation of massive radiation as exponential or power-law suppressed with string curvature depends on the specific regime and relationship between the string parameters R , δ , A and σ_d [1]. Previous work not presented here [3, 4] has shown that sinusoidal configurations in the linear regime agree with thin-string Kalb-Ramond analytic modelling. The details of this modelling are likely to be of use in GW searches for cosmic strings or the measurement of the axion spectrum from numerical simulations of axion string networks.

Acknowledgements

AD is currently supported by a Junior Research Fellowship (JRF) at Homerton College, University of Cambridge, and also performed part of this work whilst supported by an EPSRC iCASE Studentship in partnership with Intel (EP/N509620/1, Voucher 16000206). TK acknowledges funding from a University of Cambridge Centre for Mathematical Sciences Summer Bursary under the Summer

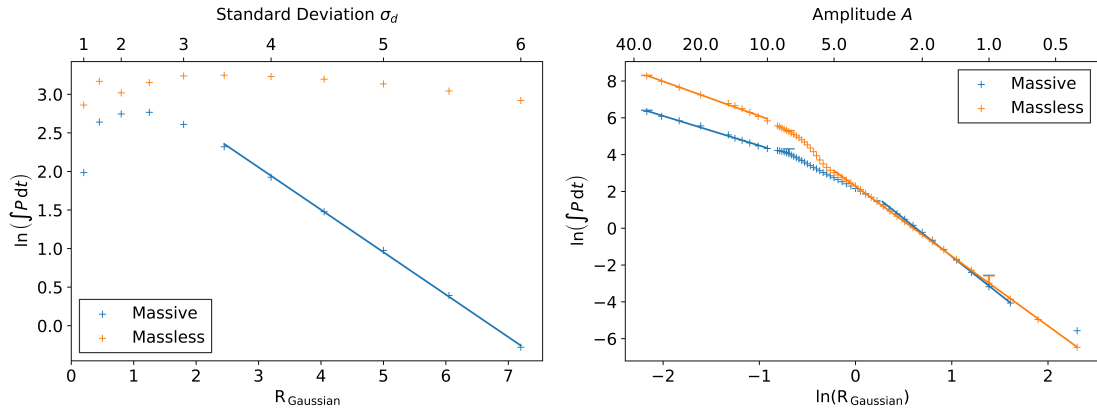


Figure 2: Massive (blue) and massless (yellow) radiation emitted from Gaussian/Gaussian collisions with amplitude $1 \leq \sigma_d \leq 6$ with $A = 5$ (left) and $0.4 \leq A \leq 35$ with $\sigma_d = 2$ (right). The plots show the time integral of the massive and massless components of the Poynting vector, P_{massive} (8) and P_{massless} (9), on the diagnostic cylinder at $R = 64$ integrated from $t = 0$ to $t = 200$.

Undergraduate Research Project scheme, as well as from STFC Consolidated Grant ST/T00049X/1. EPSS acknowledges funding from STFC Consolidated Grant No. ST/P000673/1. This article is based upon work from COST Action COSMIC WISPerS CA21106, supported by COST (European Cooperation in Science and Technology). This work was undertaken on the Fawcett supercomputer at DAMTP funded by STFC Consolidated Grant ST/P000673/1, and the Cambridge CSD3 part of the STFC DiRAC HPC Facility. The DiRAC component of CSD3 was funded by BEIS capital funding via STFC Capital Grants ST/P002307/1 and ST/R002452/1 and STFC Operations Grant ST/R00689X/1. AD and EPSS acknowledge project 2022.04048.PTDC, ‘Phi in the Sky,’ from Fundação para a Ciência e a Tecnologia (FCT), Portugal.

References

- ¹A. Drew, T. Kinowski, and E. P. S. Shellard, “Axion String Source Modelling”, <https://arxiv.org/abs/2312.07701> (2023).
- ²A. Vilenkin and E. P. S. Shellard, *Cosmic Strings and Other Topological Defects* (Cambridge University Press, July 2000).
- ³A. Drew and E. P. S. Shellard, “Radiation from global topological strings using adaptive mesh refinement: Methodology and massless modes”, *Phys. Rev. D* **105**, 063517 (2022).
- ⁴A. Drew and E. P. S. Shellard, “Radiation from global topological strings using adaptive mesh refinement: Massive modes”, *Phys. Rev. D* **107**, 043507 (2023).
- ⁵Vachaspati and T. Vachaspati, “Traveling Waves on Domain Walls and Cosmic Strings”, *Phys. Lett. B* **238**, 41–44 (1990).
- ⁶K. Clough, P. Figueras, H. Finkel, M. Kunesch, E. A. Lim, and S. Tunyasuvunakool, “GRChombo : Numerical Relativity with Adaptive Mesh Refinement”, *Class. Quant. Grav.* **32**, 245011 (2015).
- ⁷T. Andrade et al., “GRChombo: An adaptable numerical relativity code for fundamental physics”, *J. Open Source Softw.* **6**, 3703 (2021).